Analytica Chimica Acta 1056 (2019) 135–145

Contents lists available at ScienceDirect

Analytica Chimica Acta

journal homepage: www.elsevier.com/locate/aca

Electrochemical paper based cancer biosensor using iron oxide nanoparticles decorated PEDOT:PSS

Saurabh Kumar [a, b, 1], Mohammad Umar [a, 1], Anas Saifi [a], Suveen Kumar [a, c], Shine Augustine [a], Saurabh Srivastava [a, d, **], Bansi D. Malhotra [a, *]

[a] Nanobioelectronics Laboratory, Department of Biotechnology, Delhi Technological University, Shahbad Daulatpur, Delhi, 110042, India
[b] Centre for Nano Science and Engineering (CeNSE), Indian Institute of Science, Bengaluru, 560012, India
[c] Department of Chemistry, University of Delhi, Delhi, 110007, India
[d] Department of Applied Science & Humanities, Rajkiya Engineering College, Ambedkar Nagar, UP, 224122, India

HIGHLIGHTS

- PEDOT:PSS and nanostructured iron oxide modified conducting paper sensor has been reported for cancer biomarker detection.
- The electrical conductivity of the paper electrode has been enhanced by two orders of magnitude after treatment with DMSO.
- It exhibits high sensitivity of 10.2 μA $ng^{-1}mL\ cm^{-2}$ in the detection range of 4–25 $ngmL^{-1}$ for CEA detection.
- It may be a promising alternative over the expensive conventional electrodes (ITO, gold and glassy carbon).

GRAPHICAL ABSTRACT

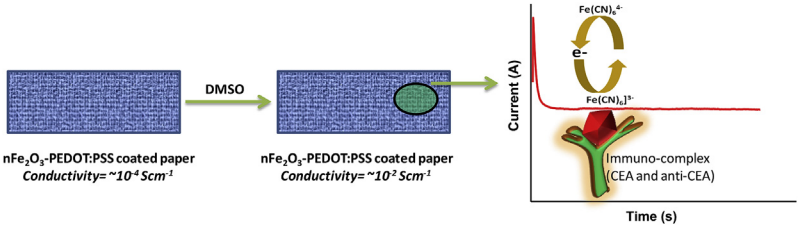

ARTICLE INFO

Article history:
Received 28 October 2018
Received in revised form
16 December 2018
Accepted 20 December 2018
Available online 8 January 2019

Keywords:
PEDOT:PSS
Iron oxide nanoparticles
Electrochemical paper
Biosensor

ABSTRACT

We report results of the studies relating to the fabrication of a label-free, flexible, light weight and disposable conducting paper based immunosensing platform comprising of poly(3,4-ethylenedioxythiophene):poly(styrenesulfonate) and nanostructured iron oxide (nFe_2O_3@PEDOT:PSS) nanocomposite for detection of carcinoembryonic antigen (CEA), a cancer biomarker. The effect of various solvents such as sorbitol, ethanol, propanol, n-methyl-2-pyrrolidone (NMP) and dimethyl sulfoxide (DMSO) on the electrical conductivity of Whatman filter paper (WP) modified with nFe_2O_3@PEDOT:PSS/WP was investigated. The electrical conductivity of the PEDOT:PSS/WP electrode was found to be enhanced by two orders of magnitude (from 6.8×10^{-4} to 1.92×10^{-2} Scm^{-1}) after its treatment with DMSO. Further, nFe_2O_3 doped PEDOT:PSS/WP electrode exhibited the electrical conductivity as 2.4×10^{-2} Scm^{-1}. Besides this, the incorporation of iron oxide nanoparticles (nFe_2O_3) into PEDOT:PSS/WP resulted in improved electrochemical performance and signal stability. This nFe_2O_3@PEDOT:PSS/WP based platform was used for immobilization of the anti-carcinoembronic antigen (anti-CEA) protein for quantitative estimation of cancer biomarker (CEA). The results of electrochemical response studies

* Corresponding author. Nanobioelectronics Laboratory, Department of Biotechnology, Delhi Technological University, Shahbad Daulatpur, Delhi, 110042, India.
** Corresponding author. Nanobioelectronics Laboratory, Department of Biotechnology, Delhi Technological University, Shahbad Daulatpur, Delhi, 110042, India.
E-mail addresses: saurabhnpl@gmail.com (S. Srivastava), bansi.malhotra@gmail.com (B.D. Malhotra).
[1] These authors contributed equally.

https://doi.org/10.1016/j.aca.2018.12.053
0003-2670/

revealed that this conducting paper based immunoelectrode had a sensitivity of 10.2 $\mu A ng^{-1} mL cm^{-2}$ in the physiological range (4–25 $ngmL^{-1}$) and shelf life of 34 days. Further, the proposed immunoelectrode was validated with conventional ELISA for the detection of CEA in serum samples of cancer patients.

1. Introduction

Paper has been used for a large number of quantitative analysis since ancient times. However, the qualitative or semi-quantitative results obtained using traditional paper-based detection methods have been reported to have limited applications [1,2]. This has been attributed to the fact that these detection methods are often dependant on the visual observations. With advancement in techniques and exploration of different materials, paper has recently been re-discovered as a sensor substrate which provides a platform for the development of paper based analytical devices [3,4]. In this context, fabrication of the conducting paper based biosensors has recently aroused much interest. Numerous materials such as metals [5], metal oxides [6], carbon nanomaterials [7,8], and conducting polymers [9,10] can be employed for fabrication of the conducting paper. Incorporation of inorganic materials such as metal and metal oxide into paper may result in improved electrical performance. However, complex processing, limited flexibility and high material cost have led to limited applications towards the fabrication of flexible conducting paper. The preparation of carbon nanomaterials necessitates tedious fabrication steps and these are known to be insoluble in most solvents making it difficult to prepare uniform films over large areas. In this context, conducting polymers are getting increased attention towards the fabrication of conducting paper as these offer good conductivity, solution processability, mechanical flexibility and are low cost [11]. Conducting polymers have conjugated π-electrons in their backbone structure and overlapping of their partially filled molecular orbitals permits the formation of delocalized molecular wave function. This allows electrons to move freely throughout the lattice [12] leading to improved electronic and optical properties [13]. Poly(3,4-ethylenedioxythiophene):poly(styrenesulfonate) (PEDOT:PSS) conducting polymer has been found to be a suitable candidate for fabrication of conducting paper owing to its uniform coating on paper while retaining the flexibility and stability [11]. Besides this, it manifests relatively high conductivity, improved electrochemical and thermal stabilities, greater transparency and good quality films can be easily coated onto desired substrates by conventional solution processing methods [14–18].

The nanostructured iron oxide has been predicted to be a promising immobilization matrix due to its fast electron-transfer kinetics, strong adsorption capacity, high surface-to-volume ratio, biocompatibility and non-toxic nature. This nano-structured material may offer suitable microenvironment for biomolecules immobilization leading to improved biosensing characteristics [19]. Moreover, a composite of PEDOT:PSS and nFe_2O_3 may provide synergistic effect resulting in the development of a flexible, lightweight, low cost and disposable biosensor. This organic-metal oxide nanohybrid (nFe_2O_3@PEDOT:PSS) modified conducting paper may facilitate improved conduction of electrons and ionic charge carriers within the hierarchical structure of cellulose paper.

Cancer is currently a major cause of mortality and medical threat worldwide. About 14 million new cases and 8.2 million cancer related deaths were reported in 2012 [20]. Carcinoembryonic antigen (CEA) is an important biomarker that can be correlated with the on-set of colorectal, ovarian, lung, pancreatic, breast and liver cancer [21]. According to a WHO report, these cancers are responsible for more than half of all deaths occurring annually [22]. Therefore, quantification of the CEA level before and after cancer treatment may facilitate early detection of this dreadful disease. Many conducting polymer based electrochemical sensors have been reported in literature for CEA detection. Zhang et al. deposited polyaniline/polypyrrole-silver dendrites composite on ITO electrode for CEA detection using electrochemiluminescence (ECL) technique and achieved a linear detection range from 0.001 to 100 $ngmL^{-1}$ in logarithmic scale [23]. Similarly an ECL based sensor was fabricated using poly(5-formylindole)/reduced graphene oxide nanocomposite (P5FIn/erGO) and obtained linear range of 0.0001–10 $ngmL^{-1}$ in logarithmic scale [24]. In another work Nie et al. deposited poly(5-formylindole)/electrochemically reduced graphene oxide (P5FIn/erGO) and gold nanoparticle composite onto ITO electrode [25]. The electrochemical response was found to be linear in the range, 0.0005 to 50 $ngmL^{-1}$. Zhao et al. reported glassy carbon electrode for CEA detection using nanocomposite of electrochemically reduced graphene oxide, gold nanoparticles (AuNPs) and poly(indole-6-carboxylic acid) [26]. These methods require additional labelling steps and/or are based on expensive conventional electrodes (ITO or glassy carbon). Due to low cost, flexible and disposable nature, conducting paper based electrochemical biosensors have been found to have many applications in smart point-of-care (POC) devices. Kumar et al. fabricated reduced graphene oxide modified conducting paper for amperometric detection of CEA [11]. This conducting paper platform had narrow linear detection range (2–8 $ngmL^{-1}$) and short shelf life (21 days). We report a facile method for the fabrication of electrochemical paper biosensor for CEA biomarker detection using iron oxide nanoparticles decorated PEDOT:PSS. The proposed electrochemical paper biosensor exhibited efficient linear detection range, high sensitivity and long term stability.

2. Experimental section

2.1. Materials

PEDOT:PSS (1.3 wt%) and biological reagents [CEA, anti-CEA, bovine serum albumin (BSA)] were procured from Sigma Aldrich. DMSO and Whatman filter paper Grade 1 were purchased from High Purity Laboratory Chemicals, India and GE healthcare, UK, respectively. Buffer and desired solutions were prepared using Milli-Q water, oleic acid capped iron oxide nanoparticles (nFe_2O_3) were received as a gift.

2.2. Fabrication of electrochemical paper electrode

An optimized amount, 10 mg of nFe_2O_3 was dispersed into 10 mL of PEDOT:PSS solution via ultrasonication method. Further, Whatman filter paper #1 (WP, 1 cm × 3 cm) was dipped into nFe_2O_3@-PEDOT:PSS solution for 1 hour followed by drying in hot air oven at 100 °C for 10 min. Thereafter, the dried paper electrode (nFe_2O_3@-PEDOT:PSS/WP) was dipped in DMSO solution for about 5 min to obtain enhanced conductivity of the paper electrode and was oven-dried at 120 °C for 5 min. The DMSO treated nFe_2O_3@PEDOT:PSS/

WP electrode was termed as the electrochemical paper (EP) electrode.

2.3. Antibody immobilization

The monoclonal carcinoembryonic antibodies (anti-CEA) were immobilized onto EP electrode via physiological adsorption. In this process 20 μl solution of anti-CEA (1000 μgmL^{-1}) in PBS (pH 7.4) was drop-cast over the surface (1×1 cm^2) of EP electrode and incubated for 6 h. It was then rinsed with PBS to remove any unbound antibodies after which the anti-CEA/EP electrode was treated with 0.1% BSA to block non-specific active sites. In this process, 20 μl solution of 0.1% BSA was drop-cast over the electrode surface, was kept undisturbed for 2 h and then rinsed with PBS. Finally, the BSA/anti-CEA/EP electrode was stored in a refrigerator at 4 °C when not in use. During electrochemical measurements, the EP electrode was dipped into the electrochemical cell up to 1 cm. Therefore the detecting area of EP electrode was $1 \times 1 cm^2$. A schematic of the fabrication electrochemical paper sensor is shown in Scheme 1.

2.4. Characterization

The prepared nanocomposite (nFe_2O_3@PEDOT:PSS) was characterized by Tecnai G2 30, ultratwin transmission electron microscopy (TEM) and by Bruker D-8 Advance, X-ray diffraction spectroscopy (Cu Kα, l = 1.5406 Å). Conductivity measurements on the various modified electrochemical papers were done using four points probe technique containing a low current source, and digital micro-voltmeter (SES Instruments, India). Surface morphology of various modified electrochemical papers electrodes was studied by an SEM (Hitachi S-3700 N) and X-ray photoelectron spectroscopy (XPS, Scientia ESCA 200). The electrochemical studies were performed on an Autolab Potentiostat/Galvanostat (Metrohm, Netherland) using a three electrode system with electrochemical paper electrode as working electrode, platinum wire as the counter electrode and silver/silver chloride (Ag/AgCl) as reference electrode in PBS (50 mM, pH 7.0) containing 5 mM $[Fe(CN)_6]^{3-/4-}$ redox species.

3. Results and discussion

3.1. Transmission electron microscopy (TEM)

Fig. 1(a) shows the transmission electron microscopy (TEM) image of nFe_2O_3 (oleic acid caped) that are nearly spherical in shape having a particle size of ~10–12 nm. However, a few of these are non-spherical or elliptical. In the TEM image of nFe_2O_3@PEDOT:PSS composite (Fig. 1(b)), the clusters of nFe_2O_3 having size of a few hundred nanometres were visible over the PEDOT: PSS substrate. However, these were not aggregated (Fig. 1(c)) and were found to be embedded and encapsulated in PEDOT:PSS polymer matrix. It appears that oleic acid capped nFe_2O_3 carrying negative charge and PEDOT being positive moieties resulted in the electrostatic adsorption of amorphous PEDOT polymer over nFe_2O_3 [27].

3.2. X-ray diffraction (XRD) studies

Fig. 1(d) shows XRD patterns obtained for (i) PEDOT:PSS, (ii) DMSO treated PEDOT:PSS and (iii) iron oxide nanoparticles doped PEDOT:PSS powder sample. The X-Ray diffraction pattern of the PEDOT:PSS showed a broad peak at $2\theta = 24.70°$ [28]. This diffraction peak perhaps arose due to PEDOT thiophene ring (π-π) stacking [29]. The DMSO treated PEDOT:PSS showed the peak shift

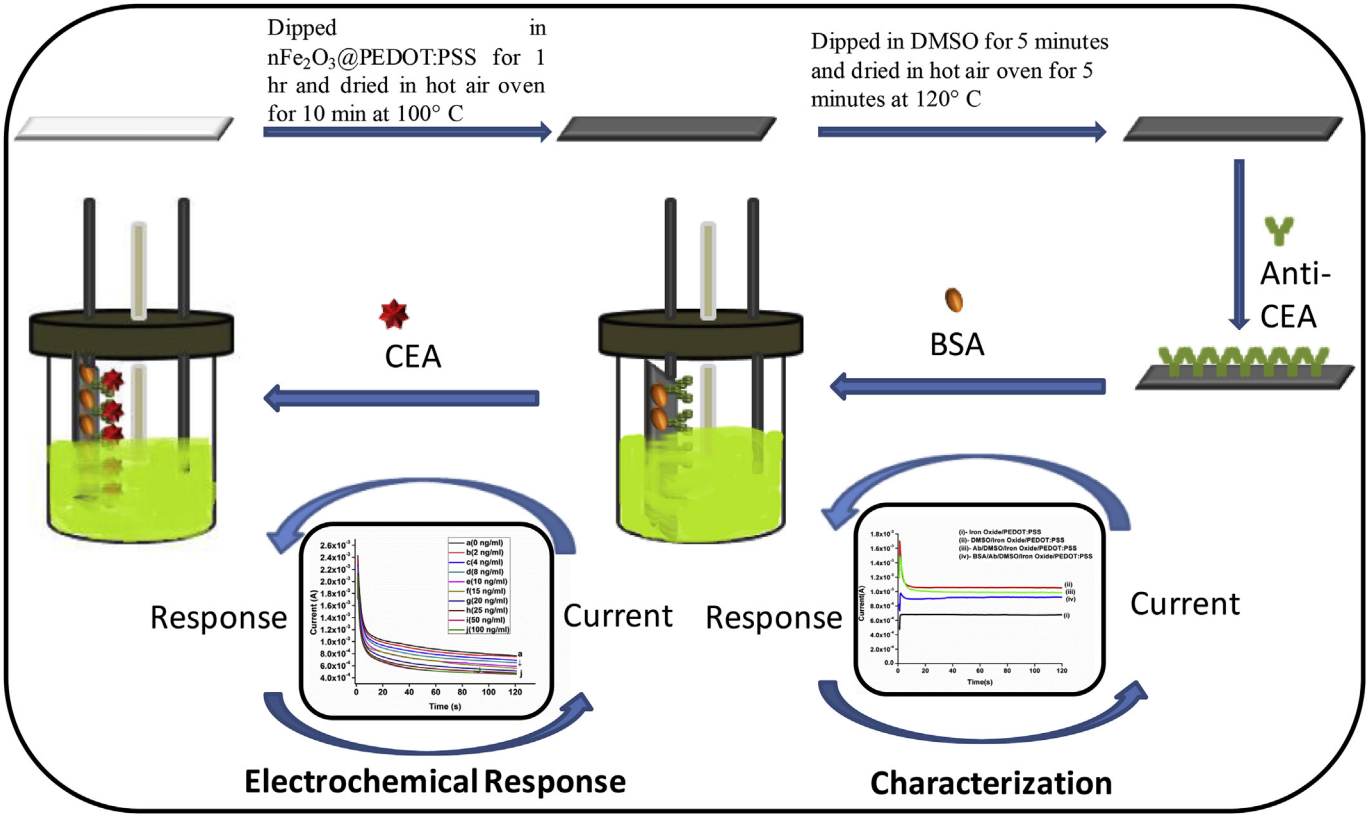

Scheme 1. Schematic representation of fabrication of electrochemical paper based cancer biosensor.

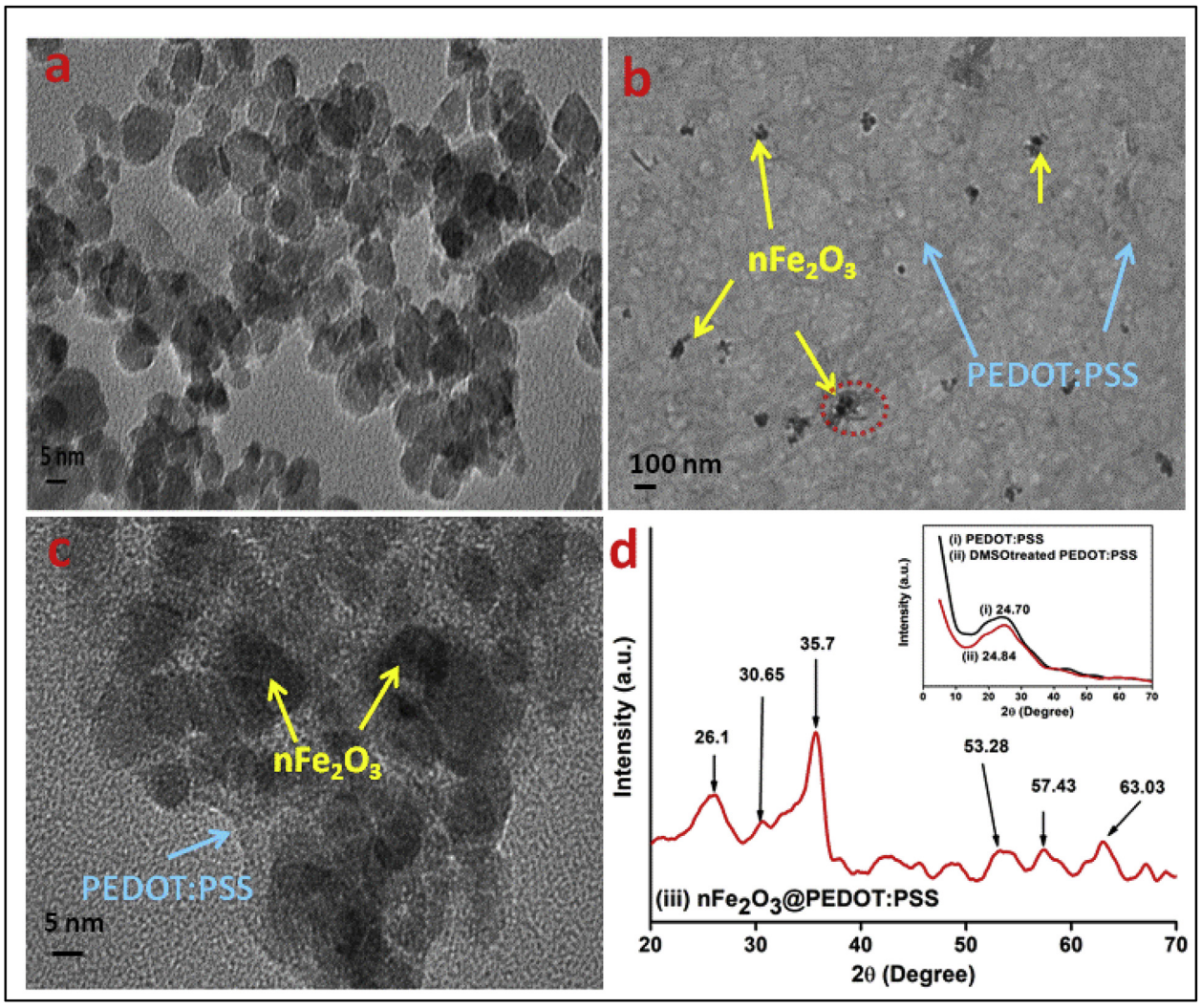

Fig. 1. TEM image of (a) nFe_2O_3, (b) nFe_2O_3@PEDOT:PSS composite, (c) enlarge view of nFe_2O_3@PEDOT:PSS composite and (d) XRD pattern of nFe_2O_3@PEDOT:PSS and the inset showing XRD of (i) PEDOT:PSS and (ii) DMSO treated PEDOT:PSS.

from $2\theta = 24.70°$ to $2\theta = 24.84°$ which corresponded to the increase in interchain planar ring stacking and a decrease in intensity was observed due to rearrangement of the crystalline domain orientation [30]. It may be noted that PEDOT is known to be highly conducting and is surrounded by non-conducting PSS molecule. After treatment with DMSO there was perhaps removal of some PSS chains from the PEDOT:PSS film [31]. That may perhaps cause conformational change in the PEDOT:PSS polymer structure. Therefore, the observed change in XRD angle (24.70° to 24.80°) indicated small conformational change and was not related to any variation of the PEDOT:PSS polymer structure. XRD of nFe_2O_3@-PEDOT:PSS showed a peak shift from 24.7 to 26.1 arising due to nFe_2O_3 entrapment in the PEDOT:PSS polymer chain. Additional peaks seen at $2\theta = 30.65$, 35.70, 53.28, 57.43, 63.03 corresponding to the (2 2 0), (3 1 1), (4 2 2), (5 1 1), (4 4 0) planes were well indexed with the standard XRD pattern of nFe_2O_3 (JCPDS No. 39–1346) [28].

3.3. Scanning electron microscopy (SEM)

The surface morphology of the electrochemical paper was examined using a scanning electron microscope (SEM). In Fig. 2(a) cellulose fibers of Whatman filter paper (WP) were clearly seen and in Fig. 2(b) PEDOT: PSS was found to be uniformly coated on WP which had perhaps smoothened the cellulose fiber. The PEDOT: PSS was largely adsorbed in/on the cellulose fibers network via capillary action. Fig. 2(c) showed small spherical moieties of nFe_2O_3 embedded in the polymer structure of PEDOT: PSS/WP (electrochemical paper, EP). Further, shiny appearance on the electrochemical paper electrode was observed (Fig. 2(d)) because of the static charge build-up arising due to non-conducting nature of the CEA antibodies which supported the immobilization of CEA antibodies. The immobilized antibodies filled up the pores and small interfiber air spaces of cellulosic network present in the nFe_2O_3/EP.

3.4. Electrical conductivity studies

The electrical conductivity of PEDOT:PSS coated paper (PEDOT:PSS/WP) was found to be ~6.8×10^{-4} Scm^{-1}. Further, we treated the PEDOT:PSS/WP electrode with different solvents and investigated its electrical conductivity (Table 1). When PEDOT:PSS/WP electrode was treated with DMSO, its electrical conductivity was improved greatly (6.8×10^{-4} to 1.92×10^{-2} Scm^{-1}) As a result, DMSO treated PEDOT:PSS/WP electrode was chosen for further studies. The reason for the increase in conductivity after DMSO treatment was attributed to the charge interaction between PEDOT and PSS which caused the reorientation of the polymer molecules

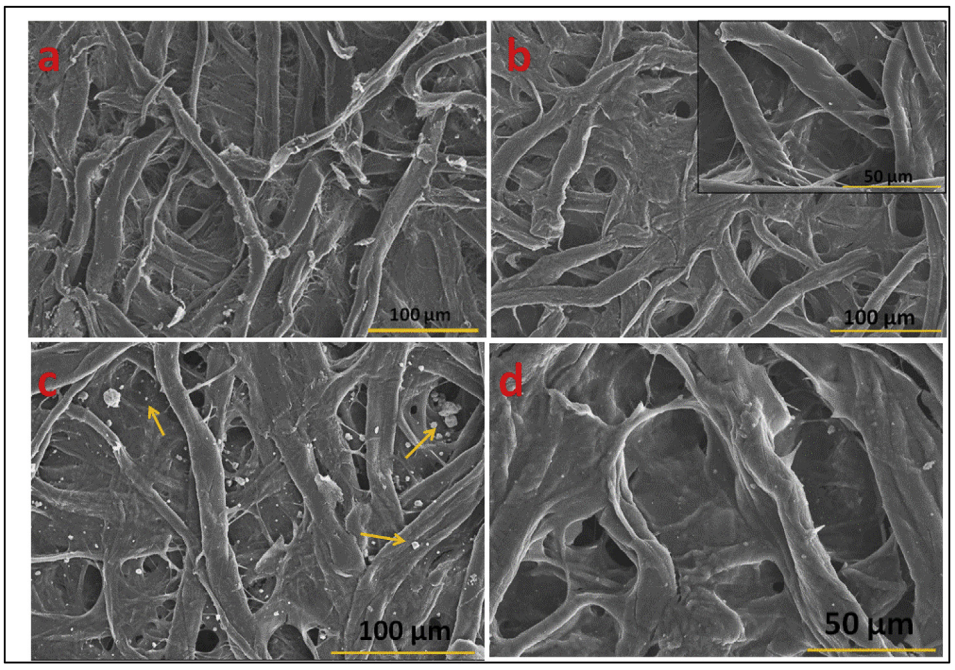

Fig. 2. SEM image of (a) Whatman filter paper (WP) (b) PEDOT: PSS/WP, (c) nFe_2O_3/PEDOT: PSS/WP (EP), (d) anti-CEA/EP.

Table 1
Effect of various solvents on the electrical conductivity of conducting paper.

S. No.	Sample	Conductivity (S/cm)
1	PEDOT:PSS coated on paper, CP	6.84×10^{-4}
2	CP dipped in N-methyl-2-pyrrolidone	6.9×10^{-4}
3	CP dipped in Sorbitol	1.3×10^{-3}
4	CP dipped in Propanol	3.6×10^{-4}
5	CP dipped in Ethanol	9.7×10^{-4}
6	CP dipped in DMSO, DMSO@CP	1.92×10^{-2}
7	nFe_2O_3/DMSO@CP (electrochemical paper, EP)	2.40×10^{-2}

enhancing the mobility of charge carriers [30]. DMSO being an aprotic solvent formed bond with hydrophobic and conducting PEDOT conjugating polymer and PSS was washed away with distilled water [31]. The PEDOT:PSS doped with iron oxide nanoparticles after treatment with DMSO (electrochemical paper) showed electrical conductivity of 2.4×10^{-2} Scm^{-1} which was nearly similar to DMSO treated PEDOT:PSS/WP.

The XPS studies were carried out to investigate the effect of DMSO treatment on PEDOT:PSS/WP electrode. The S2p core level spectra of PEDOT:PSS and DMSO treated PEDOT:PSS showed two specific peaks(Fig. 3(a)). The S2p peak present at lower binding energy (163.4 and 165.8 eV) belonged to PEDOT and S2p peak at higher binding energies (167.4 and 168.8 eV) corresponded to PSS. The doublet present in each S2p peak was due to spin orbit splitting ($2p_{3/2}$ and S $2p_{1/2}$) [32,33]. Besides this, it was found (Fig. 3(a)), that the contribution to the peak intensity of S2p from the PEDOT moiety was significantly increased after the DMSO treatment. This was due to exclusion of PSS ions upon treatment with DMSO. Further, the peak intensity ratio of PEDOT/PSS electorde increased from 0.52 to 0.69 before and after treatment with DMSO solvent, respectively. This increase was attributed to the increased contribution of the PEDOT component to the signal. Moreover, a shift in the peak of PEDOT spectra from 165.80 eV to 165.20 eV indicated that rearrangement in PEDOT structure had occurred.

Fig. 3(b) is the O1s spectra of PEDOT:PSS/WP obtained before and after its treatment with DMSO. It revealed peaks at around 533.0 and 531.27 eV that were assigned to PEDOT and PSS moieties, respectively. The peak at 531.27 eV was due to oxygen atoms bound with the sulfur atoms via double bond in the PSS chain. The peak obtained at 533.0 eV corresponded to the oxygen atom of PEDOT chain [32]. The peak intensity due to the PEDOT moietis was found to be increased after its treatment its with DMSO. The PEDOT/PSS peak intensity ratio was found to increase from 0.39 to 0.79 after the DMSO treatment, indicating removal of PSS from the conducting polymer.

3.5. Flexibility study

The flexible nature of electrochemical paper electrode was investigated by folding of the electrode in −180° to +180° fashion (Fig. 4(a)) wherein positive and negative angles indicated folding of the electrode in upward and download direction, respectively. The result was plotted as relative conductivity [ratio of measured conductivity (σ_m) to the initial conductivity (σ_o), σ_m/σ_o] against the folding angle. Fig. 4(b) shows variation in relative conductivity of electrochemical paper electrode up to 17% by folding. It can be concluded that the electrodes were flexible and there was less variation in conductivity after folding.

3.6. Electrochemical studies

The electrochemical studies of (i) nFe_2O_3/PEDOT:PSS/WP, (ii) DMSO treated nFe_2O_3/PEDOT:PSS/WP, [electrochemical paper, EP] (iii) anti-CEA immobilized over electrochemical paper [anti-CEA/EP] and (iv) BSA/anti-CEA/EP electrodes were investigated via chronoamperometric technique at regular interval of 0.1 s at a potential of 2 V (Fig. 5(a)). As shown in the figure, the electrochemical current of nFe_2O_3/PEDOT:PSS/WP electrode was observed to be ~0.65 mA. However, after treatment with DMSO the electrochemical current increased to 1.06 mA. This increase in electrochemical current was attributed to the ejection of insulating PSS ions from nFe_2O_3/PEDOT:PSS/WP electrode surface, resulting in enhanced permeability of $[Fe(CN)_6]^{3-/4-}$ redox couple [31]. After

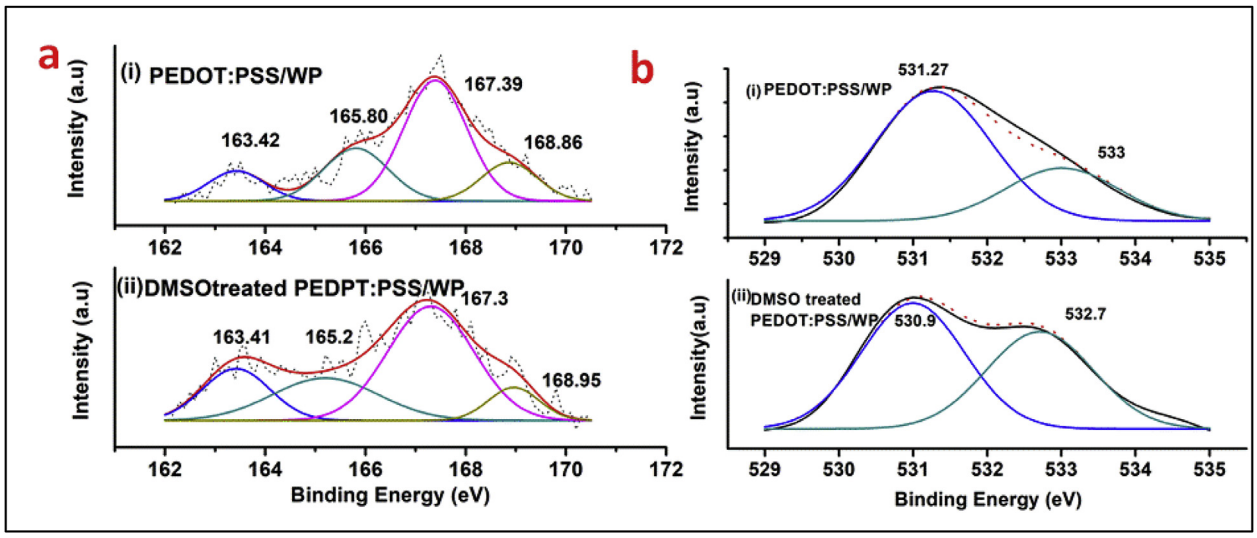

Fig. 3. XPS spectra deconvulation of a) S2p and b) O1s of PEDOT:PSS/WP and DMSO treated PEDOT:PSS/WP.

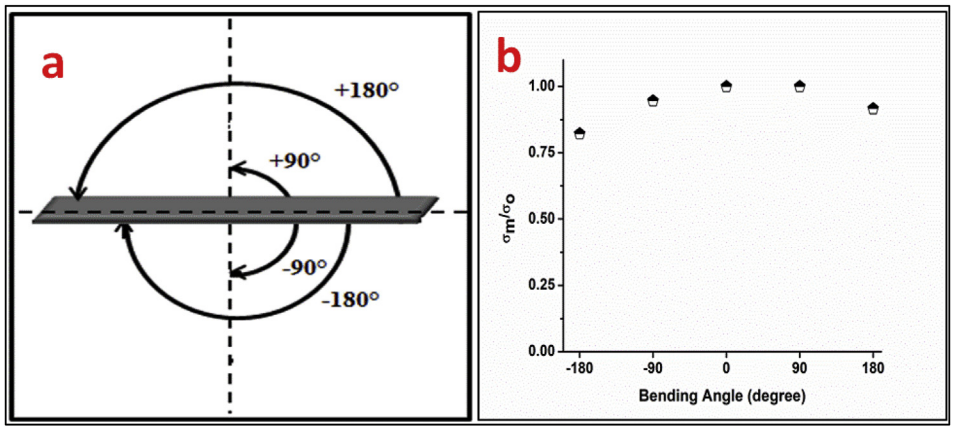

Fig. 4. **(a)** Schematic diagram of electrode folding at different angles. **(b)** Shows plot of relative conductivity vs. bending angle.

immobilization of anti-CEA onto the EP electrode the electrochemical (EC) current was found to be decreased to 0.98 mA. This decrease in EC could be due to the hindrance in electron transport at the electrode surface caused by the CEA antibodies. On treatment of anti-CEA/EP with BSA a decrease in EC current (0.92 mA) was observed due to insulating nature of BSA which hindered the electron transport [11].

Electrochemical impedance spectroscopy (EIS) was used to measure the impedance by applying small amplitude alternating current [34]. Quantification of the R_{ct} (charge transfer resistance) value of the EP electrode was done by analyzing semicircle arc of the Nyquist plot. Fig. 5 shows the Nyquist plot obtained for (b) iron oxide nanoparticles decorated PEDOT:PSS/WP (nFe_2O_3/PEDOT:PSS/WP), (c) DMSO treated nFe_2O_3/PEDOT:PSS/WP, EP electrode and (d) anti-CEA/EP in 5 mM $[Fe(CN)_6]^{3-/4-}$ containing PBS solution at the biasing potential of 0.03 V and the frequency range from 50 Hz to 100 KHz. It was observed that R_{ct} value of nFe_2O_3/PEDOT:PSS/WP (966.39 Ω, Fig. 5(b)) was found to be decreased on its treatment with high dielectric solvent DMSO (368.66 Ω, Fig. 5(c)) which diminished the coulomobic interaction between PEDOT and PSS resulting in ejection of the insulating PSS from the surface of conducting polymer [35]. This PSS ejection enhanced the exposure of inter-connected PEDOT chains resulting in enhanced $[Fe(CN)_6]^{3-/4-}$ redox probe permeability to the surface of EP electrode. After immobilization of anti-CEA onto EP electrode (anti-CEA/EP), the R_{ct} value increased to 632.08 Ω (Fig. 5(d)) due to presence of insulating surface for charge transfer [36]. Heterogeneous electron transfer rate constant (K_{ct}) of the fabricated electrodes was idetermined to delineate the electron transfer kinetics by using Eq. (1) [37]:

$$K_{ct} = RT/(n^2 F^2 A R_{ct} [S]) \quad (1)$$

where R is ideal gas constant, T is room temperature (298 K), F is Faraday constant (96485 J), A is electroactive surface area (1 cm^2), [S] is the concentration of redox probe (mol/cm^3) and n is the number of the electrons transferred per molecule of the redox probe. By using Eq. (1), K_{ct} value of the nFe_2O_3/PEDOT:PSS/WP and EP was found to be 5.51×10^{-4} and 14.45×10^{-5}, respectively. Thus, EP electrode showed increased electron transfer kinetics. The observed electrochemical properties and the conductivity of EP electrode are shown in Table 2.

3.7. Electrochemical response studies

The electrochemical response of BSA/anti-CEA/EP electrode was recorded (Fig. 6(a)) as a function of increasing concentration of CEA

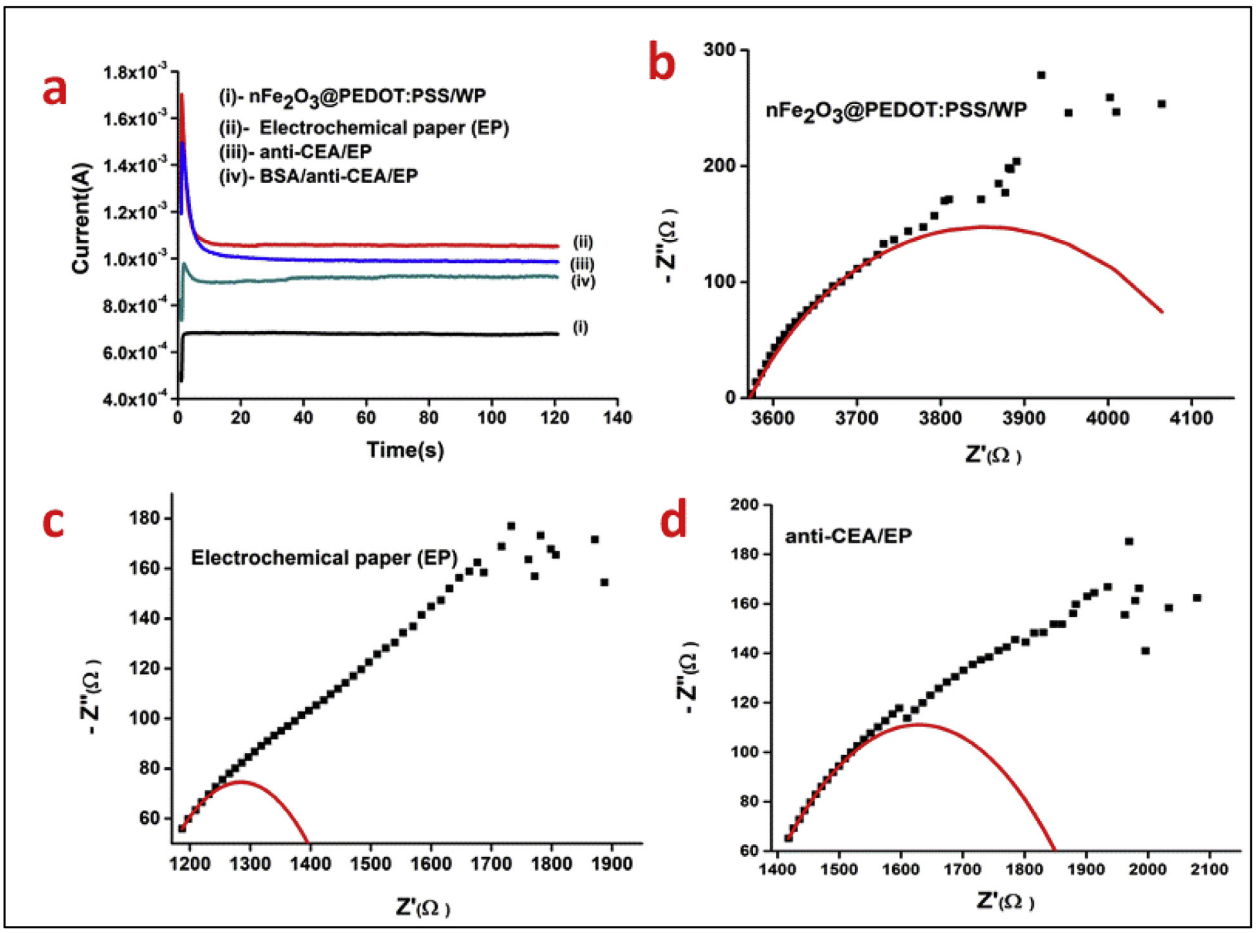

Fig. 5. (a) Chronoamperometric studies of various modified paper electrode. (b–d) EIS plot of nFe_2O_3/PEDOT:PSS/WP, electrochemical paper (EP), and anti-CEA/EP.

Table 2
Electrochemical properties of modified paper electrode.

S. No.	Electrode Surface	Conductivity (Scm^{-1})	R_{ct}	R_s	K_{ct}
1	PEDOT:PSS on Whatman filter paper [Conducting Paper (CP)]	6.84×10^{-4}	2.30 kΩ	2.16 kΩ	2.32×10^{-5}
2	nFe_2O_3/CP	9.3×10^{-3}	966.39Ω	2.12 kΩ	5.51×10^{-5}
3	nFe_2O_3/DMSO@CP (EP)	2.30×10^{-2}	368.66Ω	1.10 kΩ	14.45×10^{-5}

(2–100 $ngmL^{-1}$) in 5 mM $[Fe(CN)_6]^{-3/-4}$ containing PBS (50 mM, pH 7.0) solution using chronoamperometry with an incubation period of 10 min. The response current was found to be decreased with increase in the concentration of CEA due to the formation of electrically insulating layer of antigen-antibody complex onto the surface of fabricated biosensing electrode that perhaps hindered the electron transfer *via* the redox probe, $[Fe(CN)_6]^{3-/4-}$ at the surface of EP electrode [36]. Fig. 6(b) shows the calibration curve obtained between the CEA concentration and electrochemical response current. It was observed that the electrochemical current decreased from 2 to 25 $ngmL^{-1}$ after which the saturation in current response was observed up to 100 $ng\,mL^{-1}$. A linear detection range was obtained for CEA concentration in between 4 and 25 $ngmL^{-1}$ with sensitivity of 10.2 μAng^{-1} $mLcm^{-2}$. The linear calibration curve obeyed Eq (2).

$$I(A) = -10.2\ \mu A\ mL\ ng^{-1}\ x\ [CEA\ concentration] + 746\ \mu A;\quad R^2 = 0.95 \qquad (2)$$

The EP electrode was fabricated without nFe_2O_3 doping (with similar procedure as discussed in Section 2.2 and 2.3) and electrochemical response studies were conducted (please see supporting information, Figs. S1 and a) as a function of CEA concentration (2–100 $ngmL^{-1}$). Fig. S1,b shows the calibration curve obtained between the CEA concentration and electrochemical response current. A linear detection range was obtained for CEA concentration in between 4 and 50 $ngmL^{-1}$ with sensitivity of 2.1 $\mu Ang^{-1}mLcm^{-2}$ which is ~4.8 times lower than EP electrode performance. This confirmed that nFe_2O_3 modified EP sensor provided improved conduction of electronic and ionic charge carriers within the hierarchical structure of cellulose paper resulting in improved sensitivity.

To investigate the cross reactivity of the fabricated electrode (BSA/EP), the control studies were carried out. In this experiment, the electrochemical current response was measured against increasing concentration of the CEA antigen (Fig. 6(c)) for an electrode on which antibodies were not immobilized. No significant deviation in electrochemical current response was observed.

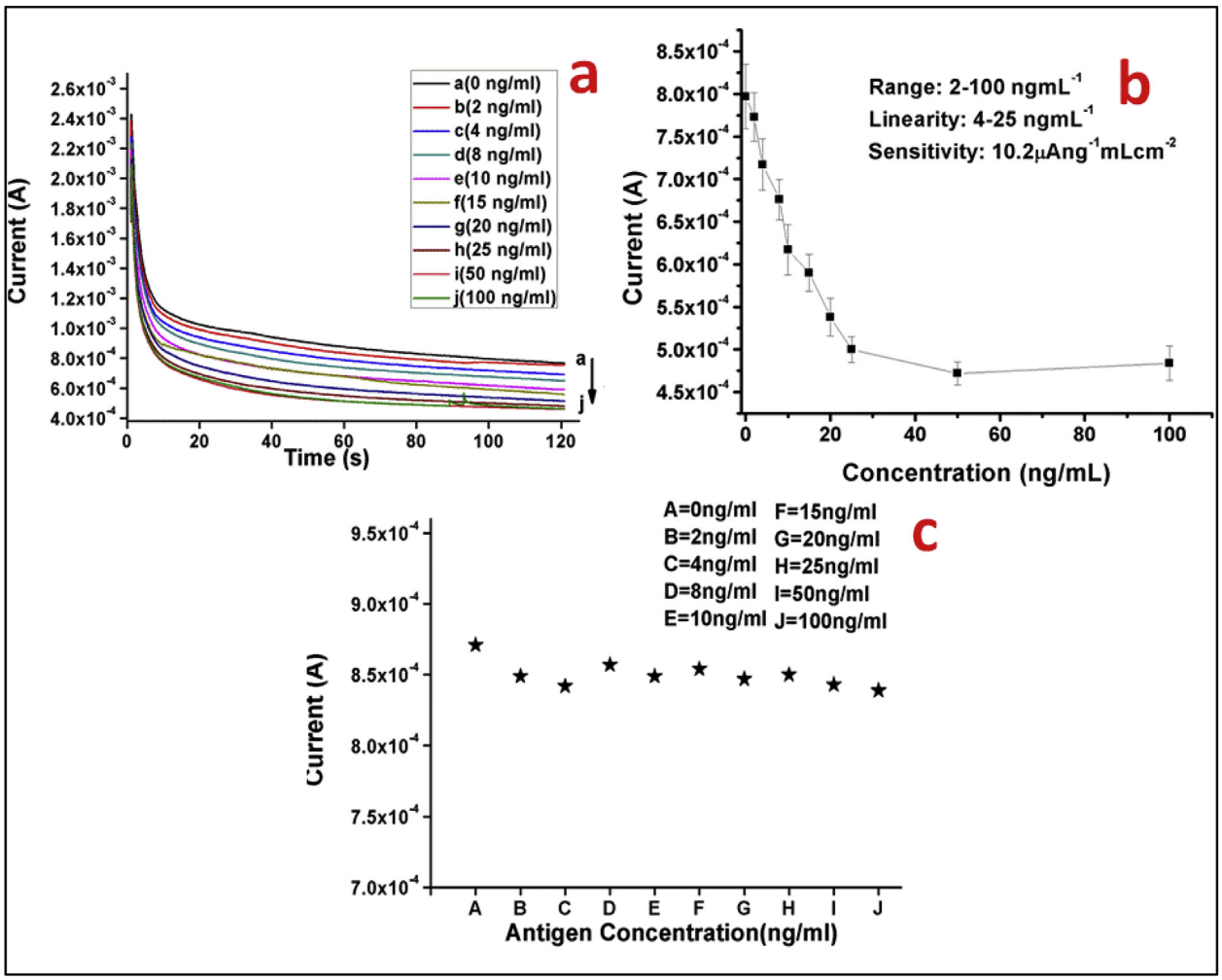

Fig. 6. **(a)** Electrochemical response studies of BSA/anti-CEA/EP electrode obtained as a function of CEA concentration (2–100 ngmL^{-1}) using chronoamperometry **(b)** Calibration plot between the magnitudes of current recorded and CEA concentration **(c)** Control study plot.

3.8. Selectivity, reproducibility and stability studies

The selectivity of the fabricated EP bioelectrode (BSA/anti-CEA/EP) was examined in the presence of cardiac troponin I (cTnI), endotheline-1 (ET-1) and cytokeratin-19 fragment (CYFRA) concentration present in normal human serum are 1 ngmL^{-1}, 2–4 pgmL^{-1} and 3.5 ngmL^{-1} respectively [38–40]. We performed interference studies even at concentration of 2 ngmL^{-1} and observed (Fig. 7(a)) no significant change in electrochemical current. And we did not find any significant change in amperometric current on addition of higher concentration of CYFRA (4 ngmL^{-1}). For the reproducibility study, the electrochemical current response of five different electrodes (BSA/anti-CEA/EP) having same surface area, fabricated under a similar set of conditions was noted in the presence of CEA concentration (2 ngmL^{-1}) [Fig. 7(b)]. This electrochemical paper electrode was found to be reproducible after the relative standard deviation of less than 5% (Mean value = 802 μA) was observed. Further, the experiments were conducted 3-times for each electrode and the error bars were included accordingly. Further, the storage stability experiment on conducting paper biosensor electrode (BSA/anti-CEA/EP) was conducted at an interval of three days (Fig. 7 (c)). It was observed that 90% activity remained upto 19 days and after 34 days the EP biosensor electrode retained the activity up to 82% when it was stored at 4 °C after which the electrochemical response current decreased to 75% in about 37 days. It can be inferred that the fabricated electrode showed reasonable good stability up to 34 days.

The characteristics of the EP based CEA biosensor were compared with those reported in literature (Table 3). This comprative study clearly revealed that Fe_2O_3/PEDOT:PSS based conducting paper (EP) showed promising detection range, sensitivity and improved shelf life as compared to other biosensors for CEA detection.

Real sample analysis was conducted to investigate the feasibility of the fabricated EP biosensor electrode (BSA/anti-CEA/EP). The blood samples of cancer patients were collected and pre-treated at RGCI&RC (Rajiv Gandhi Cancer Institute & Research Centre), Rohini, Delhi, India. Prior to conducting the real sample analysis experiments, we obtained the ethical approval from Institutional Ethical and Biosafety Committee, DTU and Institutional Review Board of RGCI&RC. The concentration of CEA present in the serum sample of cancer patients was measured using the VITROS Immunodiagnostic System. The sensitivity of EP sensor in standard and serum sample of CEA was found to be ~10.6 μAng^{-1}mLcm^{-2} and 14 μAng^{-1}mLcm^{-2} in the range of 4–20 ngmL^{-1} (Fig. S2). The sllight deviation in sensitivity of serum samples was perhaps due to the presence of other compounds present in serum samples of a person. A reasonable correlation was found between (a) CEA concentration in serum samples of cancer patients and (b) CEA concentration in standard samples as shown in Table 4.

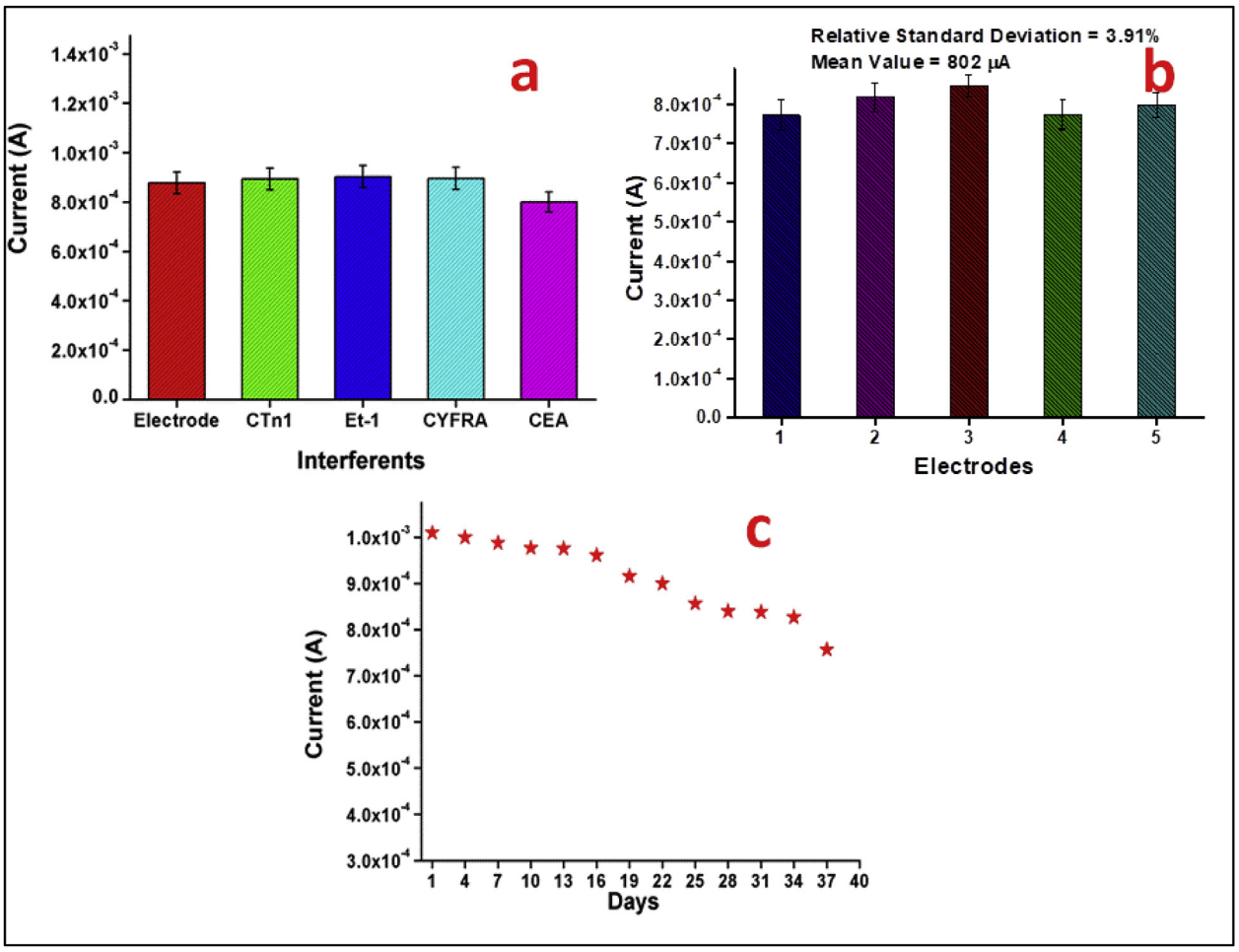

Fig. 7. **(a)** Electrochemical current response of modified electrochemical paper electrode (BSA/anti-CEA/EP, immunoelectrode) in the presence of other analytes. **(b)** Electrochemical current response of different immunoelectrode fabricated via same set of procedure **(c)** Electrochemical current response of anti-CEA immobilized immunoelectrode measured as a function of time (day).

Table 3
Comparison of present work with other electrochemical sensors reported in literature for CEA detection.

Immobilization Matrix	Fabrication Method	Detection Method	Linear Detection Range ($ngmL^{-1}$)	Sensitivity ($\mu Ang^{-1}\ mLcm^{2}$)	Shelf life (days)	Ref.
MoS_2-PBNCs	Drop casting of materials over glassy carbon electrode	Differential Pulse Voltammetry	0.005 to 10 (in log scale)	–	14	[9]
PDA/RGO	Drop casting of materials over glassy carbon electrode	Amperometry	0.0005 to 5 (in log scale)	–	30	[10]
PEDOT/IL/PANI	Drop casting of materials over glassy carbon electrode	Differential Pulse Voltammetry	0.001 to 10 (in log scale)	–	–	[11]
RGO/PEDOT:PSS	Solution processed (filter paper dip coated & treated with ethylene glycol)	Amperometry	2–8	25.8	21	[2]
CNT/PEDOT:PSS	Solution processed (filter paper dip coated & treated with formic acid)	Amperometry	2–15	7.8	18	[3]
PANI/Au	Deposition of Au on filter paper via sputtering and electrochemical deposition of PANI	Amperometry	2–20	13.9	22	[4]
PEDOT:PSS-PVA electrospun	Electrospinning of materials on conducting paper	Amperometry	0.2–25	14.2	22	[5]
Fe_2O_3/PEDOT:PSS	Solution processed (filter paper dip coated & treated with DMSO)	Amperometry	4–25	10.2	34	Present work

MoS_2: Molybdenum disulfide, PBNCs: Prussian blue nanocubes, PDA: polydopamine, RGO: Reduced graphene oxide, IL: Ionic liquid, PANI: Polyaniline, PEDOT: Poly(3,4-ethylenedioxythiophene), PSS: Polystyrene sulfonate, CNT: Carbon nanotube, Au: Gold, PVA: Polyvinyl alcohol, Fe_2O_3: iron oxide nanoparticles3.9Real sample analysis.

4. Conclusion

Nanohybrid of nFe_2O_3@PEDOT:PSS has been used to obtain a flexible, lightweight and disposable paper based electrodes. The conductivity and electrochemical studies have revealed that this electrode exhibits excellent electrical conductivity and high heterogeneous electron transfer rate constant. The nanostructured paper based electrodes has been utilized for the immobilization of anti-CEA monoclonal antibodies. The resulting immunoelectrode (BSA/anti-CEA/nFe_2O_3@PEDOT:PSS/WP) has been used for

Table 4
Determination of CEA concentration in serum samples by BSA/anti-CEA/EP electrode.

CEA Concentration ($ngmL^{-1}$)	Value of current obtained with serum sample (mA)	Value of current obtained for standard sample (mA)	% RSD
2	0.753	0.773	1.9
4	0.711	0.717	0.6
8	0.648	0.676	3
10	0.568	0.617	5.8
15	0.527	0.59	8
20	0.473	0.538	9

detection of the cancer biomarker (CEA). The proposed electrode has been found to be highly sensitive (10.2 $\mu Ang^{-1}mL\ cm^{-2}$) with good linearity in the physiological range 4–25 ng mL^{-1}. Further, a good storage stability (34 days) and applicability in real patient samples indicates the potential of this lightweight, disposable and sensitive paper based platform for smart point-of-care devices.

Acknowledgements

The authors thank Prof. Yogesh Singh, Vice Chancellor, Delhi Technological University, Delhi, India for providing the facilities. Saurabh Kumar is thankful to Prof. Shyam S. Pandey, Kyushu Institute of Technology, Japan for XPS studies and Chandra Mouli Pandey, DTU for providing iron oxide nanoparticles. S.K. is thankful to Dr. Birendra K. Yadav, Dr. D. C. Doval, Rajiv Gandhi Cancer Institute & Research Centre, Delhi, India for providing the clinical samples. Saurabh Kumar acknowledges CeNSE, Indian Institute of Science, Bengaluru, India and Department of Science and Technology, New Delhi, India for DST INSPIRE Faculty Award (DST/INSPIRE/04/2017/002750). Suveen Kumar acknowledges the Department of Science and Technology, New Delhi, India for the DST-INSPIRE Faculty Award (DST/INSPIRE/04/2017/001336). S.S. acknowledges financial assistance from the DST, New Delhi, India (Grant No. DST/INSPIRE/04/2014/002540) and AKTU, Lucknow, India (Grant under Visvesvaraya Research Promotion Scheme).

Appendix A. Supplementary data

Supplementary data to this article can be found online at https://doi.org/10.1016/j.aca.2018.12.053.

References

[1] E. Morgan, I. Wilson, An early description of paper chromatography? Chromatographia 60 (2004) 135–136.
[2] D.D. Liana, B. Raguse, J.J. Gooding, E. Chow, Recent advances in paper-based sensors, Sensors 12 (2012) 11505–11526.
[3] B. Liu, D. Du, X. Hua, X.Y. Yu, Y. Lin, Paper-based electrochemical biosensors: from test strips to paper-based microfluidics, Electroanalysis 26 (2014) 1214–1223.
[4] A.W. Martinez, S.T. Phillips, M.J. Butte, G.M. Whitesides, Patterned paper as a platform for inexpensive, low-volume, portable bioassays, Angew. Chem. Int. Ed. 46 (2007) 1318–1320.
[5] S. Gong, W. Schwalb, Y. Wang, Y. Chen, Y. Tang, J. Si, B. Shirinzadeh, W. Cheng, A wearable and highly sensitive pressure sensor with ultrathin gold nanowires, Nat. Commun. 5 (2014) 3132.
[6] A. Manekkathodi, M.Y. Lu, C.W. Wang, L.J. Chen, Direct growth of aligned zinc oxide nanorods on paper substrates for low-cost flexible electronics, Adv. Mater. 22 (2010) 4059–4063.
[7] W.J. Hyun, O.O. Park, B.D. Chin, Foldable graphene electronic circuits based on paper substrates, Adv. Mater. 25 (2013) 4729–4734.
[8] L. Wang, W. Chen, D. Xu, B.S. Shim, Y. Zhu, F. Sun, L. Liu, C. Peng, Z. Jin, C. Xu, Simple, rapid, sensitive, and versatile SWNT– paper sensor for environmental toxin detection competitive with ELISA, Nano Lett. 9 (2009) 4147–4152.
[9] S. Kumar, A. Sen, S. Kumar, S. Augustine, B.K. Yadav, S. Mishra, B.D. Malhotra, Polyaniline modified flexible conducting paper for cancer detection, Appl. Phys. Lett. 108 (2016) 203702.
[10] S. Kumar, P. Rai, J.G. Sharma, A. Sharma, B.D. Malhotra, PEDOT: PSS/PVA-nanofibers-decorated conducting paper for cancer diagnostics, Adv. Mater. Technol. 1 (2016) 1600056.
[11] S. Kumar, S. Kumar, S. Srivastava, B.K. Yadav, S.H. Lee, J.G. Sharma, D.C. Doval, B.D. Malhotra, Reduced graphene oxide modified smart conducting paper for cancer biosensor, Biosens. Bioelectron. 73 (2015) 114–122.
[12] D. Bloor, B. Movaghar, Conducting polymers, IEE Proc. Solid State Electron. Dev. 130 (1983) 225–232.
[13] M. Gerard, A. Chaubey, B. Malhotra, Application of conducting polymers to biosensors, Biosens. Bioelectron. 17 (2002) 345–359.
[14] H. Okuzaki, M. Ishihara, S. Ashizawa, Characteristics of conducting polymer transistors prepared by line patterning, Synth. Met. 137 (2003) 947–948.
[15] S. Ashizawa, Y. Shinohara, H. Shindo, Y. Watanabe, H. Okuzaki, Polymer FET with a conducting channel, Synth. Met. 153 (2005) 41–44.
[16] J. Jang, M. Chang, H. Yoon, Chemical sensors based on highly conductive poly (3, 4-ethylenedioxythiophene) nanorods, Adv. Mater. 17 (2005) 1616–1620.
[17] A.L. Briseno, M. Roberts, M.-M. Ling, H. Moon, E.J. Nemanick, Z. Bao, Patterning organic semiconductors using “dry” poly (dimethylsiloxane) elastomeric stamps for thin film transistors, J. Am. Chem. Soc. 128 (2006) 3880–3881.
[18] H. Yan, T. Kagata, Y. Mori, Y. Harashina, Y. Hara, H. Okuzaki, Micrometer-scaled channel lengths of organic field-effect transistors patterned by using PEDOT/PSS microfibers, Chem. Lett. 37 (2008) 44–45.
[19] P.R. Solanki, A. Kaushik, V.V. Agrawal, B.D. Malhotra, Nanostructured metal oxide-based biosensors, NPG Asia Mater. 3 (2011) 17–24.
[20] B. Stewart, C.P. Wild, World Cancer Report 2014, World, 2016.
[21] A.N. Bhatt, R. Mathur, A. Farooque, A. Verma, B. Dwarakanath, Cancer biomarkers-current perspectives, 132, 2010, pp. 129–149.
[22] J. Ferlay, I. Soerjomataram, M. Ervik, R. Dikshit, S. Eser, M. Rebelo, D. Parkin, D. Forman, F. Bray, GLOBOCAN 2012 v1.0, Cancer Incidence and Mortality Worldwide: IARC Cancer Base No. 11 [online], International Agency for Research on Cancer, Lyon (France), 2013.
[23] L. Zhang, Y. Wang, L. Shen, J. Yu, S. Ge, M. Yan, Electrochemiluminescence behavior of AgNCs and its application in immunosensors based on PANI/PPy-Ag dendrite-modified electrode, Analyst 142 (2017) 2587–2594.
[24] G. Nie, Y. Wang, Y. Tang, D. Zhao, Q. Guo, A graphene quantum dots based electrochemiluminescence immunosensor for carcinoembryonic antigen detection using poly (5-formylindole)/reduced graphene oxide nanocomposite, Biosens. Bioelectron. 101 (2018) 123–128.
[25] G. Nie, Y. Tang, B. Zhang, Y. Wang, Q. Guo, Label-free photoelectrochemical immunosensing platform for detection of carcinoembryonic antigen through photoactive conducting poly (5-formylindole) nanocomposite, Biosens. Bioelectron. 116 (2018) 60–66.
[26] D. Zhao, Y. Wang, G. Nie, Electrochemical immunosensor for the carcinoembryonic antigen based on a nanocomposite consisting of reduced graphene oxide, gold nanoparticles and poly (indole-6-carboxylic acid), Microchimica Acta 183 (2016) 2925–2932.
[27] C.J. Jeong, S.M. Sharker, I. In, S.Y. Park, Iron oxide@ PEDOT-based recyclable photothermal nanoparticles with poly (vinylpyrrolidone) sulfobetaines for rapid and effective antibacterial activity, ACS Appl. Mater. Interfaces 7 (2015) 9469–9478.
[28] K. Singh, A. Ohlan, P. Saini, S. Dhawan, Poly (3, 4-ethylenedioxythiophene) γ-Fe2O3 polymer composite–super paramagnetic behavior and variable range hopping 1D conduction mechanism–synthesis and characterization, Polym. Adv. Technol. 19 (2008) 229–236.
[29] K. Aasmundtveit, E. Samuelsen, O. Inganäs, L. Pettersson, T. Johansson, S. Ferrer, Structural aspects of electrochemical doping and dedoping of poly (3, 4-ethylenedioxythiophene), Synth. Met. 113 (2000) 93–97.
[30] L. Ouyang, C. Musumeci, M.J. Jafari, T. Ederth, O. Inganäs, Imaging the phase separation between PEDOT and polyelectrolytes during processing of highly conductive PEDOT: PSS films, ACS Appl. Mater. Interfaces 7 (2015) 19764–19773.
[31] T.-R. Chou, S.-H. Chen, Y.-T. Chiang, Y.-T. Lin, C.-Y. Chao, Highly conductive PEDOT: PSS films by post-treatment with dimethyl sulfoxide for ITO-free liquid crystal display, J. Mater. Chem. C 3 (2015) 3760–3766.
[32] D.A. Mengistie, M.A. Ibrahem, P.-C. Wang, C.-W. Chu, Highly conductive PEDOT: PSS treated with formic acid for ITO-free polymer solar cells, ACS Appl. Mater. Interfaces 6 (2014) 2292–2299.
[33] Y. Xia, K. Sun, J. Ouyang, Solution-processed metallic conducting polymer films as transparent electrode of optoelectronic devices, Adv. Mater. 24 (2012) 2436–2440.
[34] M. Moisel, M.L. de Mele, W.D. Müller, Biomaterial interface investigated by electrochemical impedance spectroscopy, Adv. Eng. Mater. 10 (2008) B33–B46.
[35] S. Liu, H. Deng, Y. Zhao, S. Ren, Q. Fu, The optimization of thermoelectric properties in a PEDOT: PSS thin film through post-treatment, RSC Adv. 5 (2015) 1910–1917.
[36] S. Kumar, M. Willander, J.G. Sharma, B.D. Malhotra, A solution processed carbon nanotube modified conducting paper sensor for cancer detection, J. Mater. Chem. B 3 (2015) 9305–9314.
[37] A. Bardea, E. Katz, I. Willner, Probing antigen–antibody interactions on electrode supports by the biocatalyzed precipitation of an insoluble product, Electroanalysis: Int. J. Devoted Fund. Pract. Aspect. Electroanalysis 12 (2000) 1097–1106.
[38] D. Sandil, S. Kumar, K. Arora, S. Srivastava, B. Malhotra, S. Sharma, N.K. Puri, Biofunctionalized nanostructured tungsten trioxide based sensor for cardiac

biomarker detection, Mater. Lett. 186 (2017) 202–205.
[39] E. Asham, A. Shankar, M. Loizidou, S. Fredericks, K. Miller, P. Boulos, G. Burnstock, I. Taylor, Increased endothelin-1 in colorectal cancer and reduction of tumour growth by ET A receptor antagonism, Br. J. Canc. 85 (2001) 1759.
[40] K. Okamura, K. Takayama, M. Izumi, T. Harada, K. Furuyama, Y. Nakanishi, Diagnostic value of CEA and CYFRA 21-1 tumor markers in primary lung cancer, Lung Canc. 80 (2013) 45–49.